Microbial responses to elevated temperature: Evaluating bentonite mineralogy and copper canister corrosion within the long-term stability of deep geological repositories of nuclear waste

Marcos F. Martinez-Moreno [a,*], Cristina Povedano-Priego [a], Adam D. Mumford [b], Mar Morales-Hidalgo [a], Kristel Mijnendonckx [c], Fadwa Jroundi [a], Jesus J. Ojeda [b], Mohamed L. Merroun [a]

[a] Faculty of Sciences, Department of Microbiology, University of Granada, Granada, Spain
[b] Department of Chemical Engineering, Faculty of Science and Engineering, Swansea University, Swansea, United Kingdom
[c] Microbiology Unit, Belgian Nuclear Research Centre, SCK CEN, Mol, Belgium

HIGHLIGHTS

- No bentonite illitization was observed over one-year anoxic incubation at 60 °C.
- Sulfate-Reducing Bacteria resist tyndallization and were enhanced by nutrient addition.
- Some aerobic bacteria thrive at 60 °C, while anaerobic bacteria only at 30 °C.
- Microbial diversity was reduced at 60 °C being *Pseudomonas* the dominant genus.

GRAPHICAL ABSTRACT
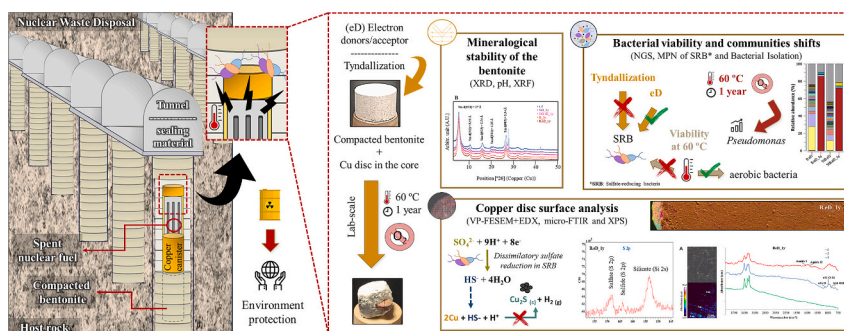
ARTICLE INFO

ABSTRACT

Deep Geological Repositories (DGRs) consist of radioactive waste contained in corrosion-resistant canisters, surrounded by compacted bentonite clay, and buried few hundred meters in a stable geological formation. The effects of bentonite microbial communities on the long-term stability of the repository should be assessed. This study explores the impact of harsh conditions (60 °C, highly-compacted bentonite, low water activity), and acetate:lactate:sulfate addition, on the evolution of microbial communities, and their effect on the bentonite mineralogy, and corrosion of copper material under anoxic conditions. No bentonite illitization was observed in the treatments, confirming its mineralogical stability as an effective barrier for future DGR. Anoxic incubation at 60 °C reduced the microbial diversity, with *Pseudomonas* as the dominant genus. Culture-dependent methods showed survival and viability at 60 °C of moderate-thermophilic aerobic bacterial isolates (e.g., *Aeribacillus*). Despite the low presence of sulfate-reducing bacteria in the bentonite blocks, we proved their survival at 30 °C but not at 60 °C. Copper disk's surface remained visually unaltered. However, in the acetate:lactate:sulfate-treated samples, sulfide/sulfate signals were detected, along with microbial-related compounds. These

* Corresponding author.
  E-mail address: mmartinezm@ugr.es (M.F. Martinez-Moreno).

findings offer new insights into the impact of high temperatures (60 °C) on the biogeochemical processes at the compacted bentonite/Cu canister interface post-repository closure.

1. Introduction

The management and safe disposal of high-level waste (HLW) containing long-lived radionuclides is a critical concern within the nuclear energy industry. To address this, HLW must be confined for over 100,000 years until it reaches natural radiation levels (Ojovan and Steinmetz, 2022). The internationally accepted option for their final disposal is the Deep Geological Repository (DGR). It consists of storing HLW in corrosion-resistant metal canisters and surrounded by a buffer material (e.g., highly compacted bentonite), as engineered barrier, and placed a few hundred meters depth within a stable geological formation, acting as natural barrier (WNA, 2021). The material of the metal canisters would depend on the DGR concept implemented by each country. Canada, Korea, Sweden or Finland has opted for, or already implemented, copper as external coating material for metal canisters (Hall et al., 2021). Compacted bentonite clay is the preferred buffer material due to its mechanical support, low permeability, strong ion exchange capabilities, self-sealing capacity, good thermal conductivity, and ideal compaction properties (García-Romero et al., 2019). Extensive geochemical, mineralogical and microbiological based research has been conducted in Spain on the bentonite from El Cortijo de Archidona site (commercialized as FEBEX) for its use in future DGRs (Martinez-Moreno et al., 2023; Povedano-Priego et al., 2021; Huertas et al., 2021; Lopez-Fernandez et al., 2014; Villar et al., 2006).

Understanding the structure and composition of the microbial community in the bentonite buffer is crucial to ensure the DGR safety. Microorganisms could impact the long-term stability of the repository, e.g., by causing microbially influenced corrosion (MIC) of the metal canisters. MIC results from processes such as biofilm formation and the production of corrosive metabolites (e.g., HS⁻). This process could induce corrosion in the canisters that would allow bacteria to interact with and mobilize radioactive materials, increasing their migration through DGR barriers (Meleshyn, 2011). Nonetheless, factors such as dry density of compacted bentonites, and heat from radioactive waste, can limit the bacterial activity.

Once the DGR is sealed, an anoxic environment will prevail due to the consumption of oxygen by microorganism or canister corrosion (Payer et al., 2019; Keech et al., 2014). The DGR microenvironment within the bentonite surrounding the metal canister will differ significantly from the host rock, transitioning from warm, dry, and oxidizing to cool, wet, and anoxic conditions (Hall et al., 2021). This microenvironment will be predominantly shaped by the thermal behavior of the canisters, which is determined by the DGR layout and the decay characteristics of the radionuclide inventory in the used nuclear fuel bundles (King et al., 2017). Under cool, wet and anoxic conditions, certain anaerobic bacteria (e.g., sulfate-reducing, SRB; and iron-reducing bacteria, IRB) can be potentially active. These bacteria could induce MIC, reduce the structural iron in smectite (the main mineral in bentonites), and metabolize sulfate to sulfide (the main corrosion agent of copper). For instance, *Desulfovibrio vulgaris* and *Desulfitobacterium frappieri* cause MIC by reducing the structural Fe(III) in smectite, and generating sulfide, through sulfate reduction (Pentráková et al., 2013; Liu et al., 2012; Shelobolina et al., 2003). The presence of sulfide in the DGR will be primarily due to SRB activity (Bengtsson and Pedersen, 2017). Sulfide can diffuse through the buffer materials, reaching the canister surface and resulting in the corrosion of copper. Another important aspect to consider is the compaction density of the bentonite. While there is no clear dry-compaction density threshold for the presence of SRB, research indicated that their growth and multiplication are more pronounced at lower compaction densities compared to higher densities, surviving in a metabolically inactive or spore-forming state to cope with the harsh

environmental conditions (Bengtsson and Pedersen, 2017, 2016). Previous studies have reported that no significant differences at the microbial community level were observed between 1.5 and 1.7 g cm⁻³ of dry density in the Spanish bentonite after two years of anaerobic incubation, while detecting SRB such as *Desulfuromonas*, *Desulfosporosinus*, and *Desulfovibrio* (Povedano-Priego et al., 2021). Moreover, Martinez-Moreno et al. (2023) demonstrated the survival of SRB in bentonite with a dry compaction density of 1.7 g cm⁻³ after one year of anoxic incubation at 30 °C and their potential effect on the corrosion of copper material. Previous studies have investigated the impact of microbial activity on canister materials and the stability of commercial bentonites such as MX-80, Opalinus Clay, and FEBEX (Pedersen, 2010; Smart et al., 2017; Martinez-Moreno et al., 2023; Madina et al., 2005). Temperature is another critical physical parameter to be considered in the DGR safety studies. The temperature evolution on the surface of the canisters will depend on the DGR concept, location, and the materials used as engineered barriers. The Canadian program (based on copper-coated canister) predicts a temperature evolution rising to a maximum peak of around 100 °C within several decades, followed by a gradual decrease to ambient temperature (King et al., 2017).

Therefore, the present study attempts to explore the impact of high temperature (60 °C) and bentonite dry-compaction density on the evolution of microbial communities, corrosion of copper surface, and the stability of the bentonite's mineralogy at the copper canister/compacted bentonite interface under anoxic conditions. To approach a more realistic scenario, simulating a post-closure DGR stage, highly compacted bentonite blocks (1.7 g cm⁻³), with high-purity copper disks in the core, were elaborated. The study examined the one-year anaerobic evolution of microbial communities at 60 °C, with one set of bentonites supplemented with acetate, lactate, and sulfate as electron donors and acceptor to stimulate indigenous bentonite bacteria (e.g., SRB). State-of-the-art microscopic and spectroscopic techniques were employed to assess the stability of the bentonite and the potential corrosion of copper disks. The survival of SRB was quantified through the most probable number (MPN) method. However, to the best of our knowledge, this is the first study to comprehensively describe the behavior of indigenous bacteria from highly compacted Spanish bentonite on the mineralogical stability of clay and copper corrosion at high temperatures (60 °C) simulating the first period in the DGR.

2. Material and methods

2.1. Bentonite source and pre-treatment

The bentonite used in this work was collected from El Cortijo de Archidona located in the southeastern region of Spain, specifically in Almeria. Samples were aseptically collected in February 2020, at a maximum depth of ~80 cm. Once in the laboratory, bentonite was manually disaggregated and dried in a laminar flow cabinet for at least 5 days at room temperature. Following the removal of excess moisture, the bentonite was meticulously ground using a sterile stainless-steel roller and mortar to achieve a homogeneous powder. Subsequently, it was carefully stored at 4 °C until it was needed for further analysis.

The samples' treatments were previously described in Martinez-Moreno et al. (2023). Briefly, sterile solutions of sodium acetate (30 mM), sodium lactate (10 mM), and sodium sulfate (20 mM) were sprayed on the bentonite to stimulate the activity of anaerobic bacteria, such as SRB. Control samples were only supplemented with sterile distilled water. The solutions were gradually added until reaching a bentonite with mud-like consistency. Then, they were dried at room temperature and ground under sterile conditions until homogeneous

powder was achieved. In addition, another set of bentonite samples underwent a heat-shocking process known as tyndallization (110 °C for 45 min, 3 consecutive days), hereinafter referred to as "sterilized bentonite", aimed at reducing the presence and activity of indigenous bacteria within the bentonite. The description of the different treatments is summarized in Table 1.

2.2. Assembly of compacted bentonite blocks with copper disks

The bentonite blocks assembly was conducted in the Laboratorio de Mecánica de Suelos (CIEMAT. Madrid, Spain) as explained in detail by Martinez-Moreno et al. (2023). In order to achieve a dry density of 1.7 g cm^{-3}, the quantity of bentonite was determined considering the initial moisture percentage (12 %), the volume of the cylindrical steel mold (dimensions of 30.3 × 20.0 mm), and the volume of the copper disks (0.31 cm^3). The initial degree of saturation of the bentonite was approximately 55 %, based on the initial moisture content (12 %), the dry density (1.7 g cm^{-3}), and the specific gravity of the FEBEX bentonite (2.7 g cm^{-3}). The saturated moisture content was estimated to be around 21 %, corresponding to a water activity (aw) of 0.94–0.95 or a Relative Humidity (RH) of 94–95 % (Fernández, 2004). Then, a pressure of 25–30 MPa was applied with a hydraulic press to achieve the desired compaction.

Oxygen-free high conductivity (OFHC) copper disks were acquired from Goodfellow company (https://www.goodfellow.com). The copper grade was C101 (purity: 99.9–100 %) with dimension of 4.0 ± 10 % mm thickness and 10.0 ± 0.5 mm diameter. Cu disks were sterilized by autoclaving for 15 min at 121 °C and placed in the core of the bentonite blocks. The resulting blocks were placed into an anaerobic jar containing an anaerobiosis generator sachet (AnaeroGen™, Thermo Scientific), and were incubated at 60 °C for one year to simulate the early stages within the DGR after its closure.

2.3. Mineralogical and geochemical analyses of the bentonite

After incubation, the samples were shattered using a sterilized stainless-steel spatula and ground with an aseptic mortar until a homogeneous powder was achieved.

Mineralogical characterization was carried out by XRD analysis through oriented aggregates (OA) technique to examine the behavior of the basal reflections of smectite under different treatments. The sample preparation (a mixture of the three replicates) was performed following the procedure described in Martinez-Moreno et al. (2023). OA samples were analyzed by a powder X-ray diffraction by a PANalytical X'Pert Pro diffractometer equipped with an X'Celerator solid-state linear detector, employing CuKα radiation at 45 kV and 40 mA. Data collection involved a step increment of 0.008° 2Θ and a counting time of 10 s/step. Subsequently, the samples were exposed to ethylene-glycol (EG) vapor at 60 °C for 24 h, and re-analyzed using the same parameters. The XRD diffractograms were analyzed utilizing the HighScore software.

The elemental composition of the bentonite from the different treatments (a mixture of the three replicates) was assessed through X-ray fluorescence (XRF) analysis using a PANalytical Zeltium instrument. The analysis employed a rhodium anode ceramic X-ray tube equipped with an ultra-thin high transmission beryllium front window.

The pH of the bentonite samples was determined in triplicate following the method described in Povedano-Priego et al. (2019). The bentonite was mixed and homogenized with 0.01 M CaCl$_2$ at a ratio of 1:15.

2.4. Characterization of bentonite microbial communities

Following a year of anaerobic incubation, the bentonite samples were preserved at −20 °C for the investigation of the bacterial diversity. Simultaneously, for culture-dependent techniques, separate samples were maintained at 4 °C. To perform these analyses, the bentonite blocks were first broken into small fragments, and then finely ground into a homogeneous mixture using a sterile mortar.

2.4.1. Total DNA extraction and 16S rRNA gene sequencing

DNA extractions were conducted, in triplicate for each treatment (B. eD, B, StB.eD, StB) and incubation time (t. 0 and after 1-year incubation at 60 °C), following the optimized phenol-chloroform-based protocol described by Povedano-Priego et al. (2021), with some modifications. In the first steps, bentonite powder was moistened with sterile milliQ water in a ratio of 1:3 w/v and stored at 4 °C for at least 3 days. Subsequently, 0.3 g of the bentonite sample was placed into 2 mL screw-cap tubes, along with sterilized glass beads. The total amount of bentonite used per replicate varied depending on the samples, ranging from 3.6 g to 10.8 g, in order to achieve good DNA yields for sequencing purposes. Afterwards, 400 μL of Na$_2$HPO$_4$ (0.12 M) was added to each tube and then vortexed at a maximum speed. Subsequently, the chemical lysis was achieved by adding 650 μL lysis buffer, 28 μL lysozyme (10 mg/mL), and 4 μL proteinase K (20 mg/mL). After performing the bead beating at a speed of 5.5 m s^{-1} for 45 s three times, the samples were incubated 45 min at 37 °C followed by an incubation at 60 °C for 75 min. Finally, the next steps of the protocol were followed in detail as described in Povedano-Priego et al. (2021). The total DNA obtained was quantified on a Qubit 3.0 Fluorometer (Life Technology, Invitrogen™).

Amplification of the extracted DNA, sequencing, and the bioinformatics analyses were performed at STAB VIDA (Caparica, Portugal, https://www.stabvida.com) and are detailed in Martinez-Moreno et al. (2023). For library construction, the primers pair 341F - 785R were employed, targeting the V3-V4 variable regions of 16S rRNA gene (Thijs et al., 2017). Sequencing was performed on the Illumina MiSeq platform and the resulting raw sequence data were then analyzed using QIIME2 v2023.2 (Caporaso et al., 2010). The reads were grouped into operational taxonomic units (OTUs) and taxonomically classified using the scikit-learn classifier with the SILVA database (release 138 QIIME). The raw data were submitted to the sequence read archive (SRA) at the National Center for Biotechnology Information (NCBI) under the BioProject accession number PRJNA1044717.

Explicet 2.10.5 (Robertson et al., 2013) was used to obtain alpha diversity indices and conduct analysis of the relative abundance of the annotated different taxa. To assess the similarity between samples at the genus level, a matrix based on the Bray-Curtis algorithm was generated and then subjected to PCoA (Principal Coordinate Analysis) using the Past4 software (Hammer and Harper, 2001).

Table 1

Sample ID and description of the treatments of the bentonite blocks. All samples were compacted to 1.7 g cm^{-3} dry density containing an oxygen-free high conductivity (OFHC) copper disk (Cu disk) in the core. Bentonite blocks were incubated 1 year at 60 °C under anaerobic conditions.

Sample ID	Treatment
B.eD_1y	Bentonite amended with acetate, lactate and sulfate (30:10:20 mM)
B_1y	Bentonite amended with distilled water
StB.eD_1y	Sterilized bentonite amended with acetate, lactate and sulfate (30:10:20 mM)
StB_1y	Sterilized bentonite amended with distilled water

Glossary: B: bentonite, StB: sterilized bentonite, eD: treated with electron donors and sulfate.

2.4.2. Determination of the most probable number of sulfate-reducing bacteria

In order to assess the impact of the temperature and the electron donors/acceptor addition on bacteria involved in copper corrosion, the number of culturable SRB was estimated by the Most Probable Number (MPN) enumeration method. This method was performed following the MPN Method of Biotechnology Solutions (Houston, USA, https://biotechnologysolutions.com), based on serial dilution in triplicate, in Postgate medium (DSMZ_Medium63, https://www.dsmz.de) replacing Na-thioglycolate with Cysteine-HCl (0.5 g L^{-1}). The procedure was conducted under anoxic conditions within an Argon-atmosphere glove box. For each treatment, 10 mL of N$_2$-degassed phosphate-buffered saline solution (PBS) was mixed with 1 g of anoxically-ground bentonite from the 3 block replicates per treatment. To facilitate the detachment of bacterial cells from the bentonite particles, the mixtures were shaken at 180 rpm for 24 h. Subsequently, 0.5 mL of the suspension was transferred to 4.5 mL of the modified Postgate medium in N$_2$-degassed septum bottles until the 10^{-5} dilution. Afterwards, the septum bottles were sealed and incubated at 30 °C and 60 °C in static and darkness conditions for 4 weeks. This process was carried out in triplicate for each treatment. The MPN of SRB was estimated by comparing positive bottles (presence of black precipitates) to a reference table (MPN Method, https://biotechnologysolutions.com), considering the initial pre-dilution for the cell's dispersion (1 g of bentonite in 10 mL of PBS).

2.4.3. Isolation and molecular identification of thermophilic-aerobic bacteria and anaerobic bacteria

For the aerobic bacterial isolation, 1 g of ground bentonite (a mixture of the three replicates) was added to 10 mL of PBS and shaken to facilitate the cell separation. For thermophilic bacteria, oligotrophic R2A medium (Reasoner and Geldreich, 1985) and 10 % Luria-Bertani (LB) medium (Miller, 1972) were used. Subsequently, 100 μL from the mixtures (bentonite + PBS) and from the positive MPN bottles, for the isolation of anaerobic bacteria, were spread on their corresponding agar media, which were sealed with parafilm, and incubated at 60 °C. The modified-Postgate agar plates were incubated at 30 °C and 60 °C under anoxic conditions within an anaerobic jar. Once growth was detected, isolated colonies were regrown until pure cultures were obtained by morphological and microscopic observation of the colonies.

DNA extraction from the pure cultures was performed with 100 μL of PrepMan™ Ultra Sample Preparation Reagent (Thermo Fisher) heating the samples 10 min at 95 °C. The 16S rRNA gene fragments amplification was performed using the primer pair 341F (5′-TCGTCGGCAGCGT-CAGATGTGTATAAGAGACAGCCTACGGGNGGCWGCAG-3′) and 785R (5′-GTCTCGTGGGCTCGGAGATGTGTATAAGAGA-CAGGACTACHVGGGTATCTAATCC-3′). The PCR (Polymerase Chain Reaction) reaction proceeded as one initial cycle at 94 °C for 2 min, followed by 30 cycles of 94 °C for 30 s, 56 °C for 30 s, and 72 °C for 2 min. Concluding, there was a final extension step at 72 °C for 10 min. The PCR products were purified using Wizard® SV Gel and PCR Clean-Up System (Promega). The purified products were sequenced to Sanger Sequencing (Eurofins Genomics, Germany). The resulting sequences were classified with The RDP Classifier and compared with those available in the GenBank by BLAST (Basic Local Alignment Search Tool) analysis. The nucleotide sequences reported here were submitted to the sequence read archive (SRA) at the National Center for Biotechnology Information (NCBI) under the BioProject accession number PRJNA1045398.

2.5. Assessment of the copper disk surface corrosion

The copper disks were extracted from the bentonite blocks and prepared for VP-FESEM (Variable Pressure-Field Emission Scanning Electron Microscopy) coupled with EDX (Energy-Dispersive X-ray) analysis. The preparation was conducted as described in Martinez-Moreno et al. (2023). Briefly, the disks were immersed in 2.5 %

glutaraldehyde in 0.1 M PBS buffer (24 h at 4 °C), washed in the same buffer 3 times (15 min. each), and post-fixed in 1 % osmium tetroxide (1 h at room temperature). Lastly, they were subjected to Critical Point Drying technique (Anderson, 1951) employing carbon dioxide in a Leica EM CPD300 instrument followed by carbon coating through evaporation utilizing an EMITECH K975X Carbon Evaporator.

For the spectroscopic analyses of the Cu surface, samples were removed from the bentonite blocks without further preparation or cleaning of the copper surface (unmodified). Reflectance micro-Fourier Transform Infrared Spectroscopy (micro-FTIR) was employed for the detection of organic compounds on the copper disk surfaces, using a PerkinElmer Spotlight micro-FTIR spectroscope equipped with a mercury-cadmium-telluride detector (16 gold-wired infrared detector elements). Reflectance micro-FTIR images were collected using a per-pixel aperture size of 25 μm × 25 μm, four scans per pixel, and a spectral resolution of 16 cm^{-1}.

Additionally, the surfaces of the unmodified copper disks were chemically analyzed by X-ray Photoelectron Spectroscopy (XPS) using a Kratos AXIS Supra Photoelectron Spectrometer. The X-ray source was a monochromated Al Kα (1486.6 eV) operating at an X-ray emission current of 20 mA and an anode high tension (acceleration voltage) of 15 kV. The take-off angle was fixed at 90° relative to the sample plane. Data was gathered from three randomly selected positions, with each acquisition area forming an approximately 110 μm × 110 μm rectangle (FOV2 lens). Analysis comprised a broad survey scan (pass energy of 160 eV, step size of 1.0 eV) and a high-resolution scan (pass energy of 20 eV, step size of 0.1 eV) for component speciation. The integral Kratos charge neutralizer served as an electron source to counteract differential charging. The binding energy scale was calibrated using the Au 4f$_{5/2}$ (83.9 eV), Cu 2p$_{3/2}$ (932.7 eV) and Ag 3d$_{5/2}$ (368.27 eV) lines of cleaned gold, copper and silver standards from the National Physical Laboratory (NPL), UK. CasaXPS 2.3.22 (Fairley, 2019) software was employed to fit the XPS spectra peaks. The effect of surface charging was compensated for all the binding energies by referring to the C 1s adventitious carbon peak at 285 eV. There were no further restrictions applied on the initial binding energy values.

3. Results and discussion

3.1. Analyses of the mineralogical and chemical stability of the bentonite

The Spanish bentonite from El Cortijo de Archidona, commercialized as FEBEX clay, has been chosen by ENRESA, the Spanish national radioactive waste company, as the preferred backfilling and sealing material the future DGR in Spain. This clay has been extensively studied under the FEBEX project since the 90s (Huertas et al., 2021). Despite the comprehensive physicochemical characterization of this bentonite, there is a growing necessity to unravel the ways by which microorganisms could impact the safety of the different DGR barriers.

The pH values and the chemical characterization by XRF are shown in Supplementary Table S1. The pH from the different treatments showed no remarkable differences after one year of anoxic incubation at 60 °C. The chemical characterization showed that the dominant oxides were SiO$_2$ and Al$_2$O$_3$ with no important differences among the treatments. After one year of incubation, slight increases (Δ) were detected in the percentage of Fe, Na, and Al oxides (Δ 1.27 %, Δ 1.25 %, and Δ 1.04 %, respectively) and decreases (negative Δ) in the concentration of Si and Mg oxides (Δ −3.27 % and Δ −0.47 %, respectively), on average. The chemical composition of the bentonite from this study closely aligns with the BI-2 sampling site in Cortijo de Archidona reported by Lopez-Fernandez et al. (2014).

Although the aim of this study does not delve into an exhaustive examination of the stability of the physico-chemical parameters of bentonite samples, it is important to consider the impact of microorganisms on the safety-relevant characteristics of the clay. Meleshyn (2011) outlined the potential influence of microbial activity on clay
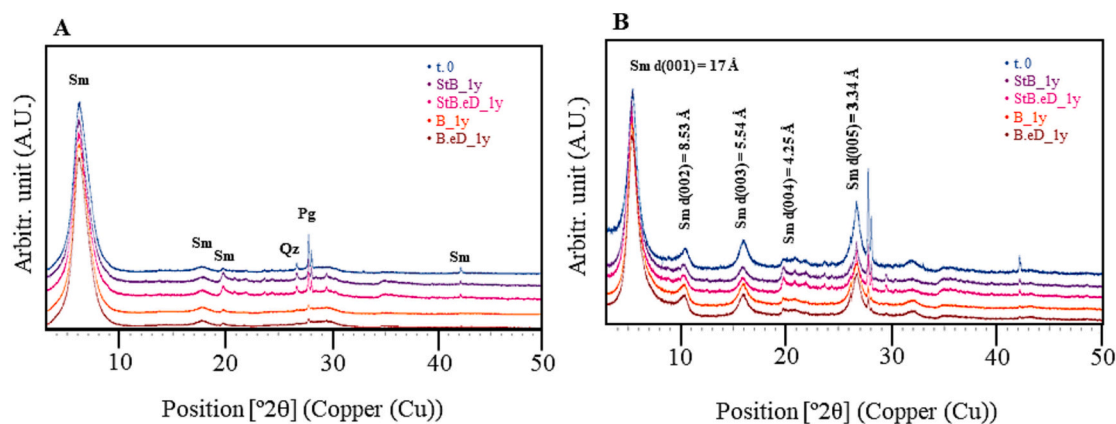
Fig. 1. (A): Oriented aggregates (OA) X-ray diffraction (XRD) patterns of samples at t. 0 and after one year of anaerobic incubation at 60 °C (1y). (B): OA XRD spectra after 24 h of exposure to ethylene glycol (EG) at 60 °C. Glossary: B: bentonite, StB: sterilized bentonite, eD: addition of acetate, sulfate, and lactate. Sm: smectite; Qz: quartz; Pg: plagioclase.

Table 2
Most probable number (MPN) of SRB per gram of bentonite (MPN g^{-1}). The values were obtained taking into account the initial pre-dilution for the cell's dispersion (1 g of bentonite in 10 mL of PBS). Glossary: t. 0: initial bentonite sample; B: bentonite; StB: sterilized bentonite; eD: addition of acetate, lactate, and sulfate; _1y: after one year of anaerobic incubation at 60 °C.

Sample	XYZ pattern[a]	MPN reading[b]	3PB dilution[c]	MPN mL^{-1}	MPN g^{-1} bentonite
t. 0	330	25.0	10^0	25.0×10^0	2.5×10^2
B_1y	210	1.5	10^{-2}	1.5×10^2	1.5×10^3
B.eD_1y	330	25.0	10^{-1}	25.0×10^1	2.5×10^3
StB_1y	320	9.5	10^0	9.5×10^0	9.5×10^1
StB.eD_1y	210	1.5	10^{-1}	1.5×10^1	1.5×10^2

[a] XYZ pattern: number of positive bottles after 3PB dilution.
[b] MPN reading: MNP value from the reference table.
[c] 3PB dilution: dilution with 3 positive bottles prior to XYZ pattern.

properties (e.g., swelling pressure, specific surface area, cation exchange capacity, anion sorption capacity, among others), affecting the stability of bentonite and, in consequence, the DGR safety. Microbial processes that could compromise the integrity of the clay encompassed actions such as the reduction and dissolution of clay minerals, the formation of biofilms, a hydrogen sulfide attack by SRB, and the generation of microbial gases. One concern is the irreversible smectite-to-illite transformation, which impacts the swelling capacity (Kaufhold and Dohrmann, 2010). This transformation is often driven by high temperatures (100–200 °C) and time, but can also occur at lower temperatures (<50 °C) (Ohazuruike and Lee, 2023). Illitization could be triggered by K$^+$ (possibly from K-feldspars of the clay) that attach to the smectite interlayer and bond covalently with oxygen (Kaufhold and Dohrmann, 2010). However, the smectite-to-illite transformation process could be stimulated by microbial activity affecting the geochemical conditions. Certain bacteria, i.e., IRB and SRB could use the structural Fe(III) in smectite as electron acceptor associated with the oxidation of organic matter or H$_2$, leading to the illite formation (Kim et al., 2019).

In our study, XRD patterns showed that the dominant mineral phase was smectite (montmorillonite), besides minor mineral phases as quartz and plagioclases (Fig. 1_A). These results are in agreement with those of previous studies which reported that the mineral composition of this bentonite consists of smectites (montmorillonite) as the dominant mineral phase (~ 84 %), followed by plagioclase (albite) and quartz (about 12 % and 3 %, respectively) (Lopez-Fernandez et al., 2015; Povedano-Priego et al., 2019). The dioctahedral smectites maintain bentonite ability to expand, as indicated for all samples by the (001) reflection at around 17 Å in the ethylene glycol (EG) pattern (Fig. 1_B), confirming the full expansion of interlayer sites without undergoing illitization (Fernández et al., 2022). Indeed, under the essayed conditions (e.g., addition of electron donors/acceptor, tyndallization process, anoxic conditions, incubation at 60 °C, etc.), no illite was detected.

Moreover, no appreciable differences in the mineralogy were observed between treatments after one year of incubation. Hence, the stability of the smectite remained unaffected by both biotic and abiotic factors at 60 °C. Although one year might be considered a relatively short time for detecting the conversion from smectite to illite in the samples, it remains essential to investigate its presence in the bentonite samples, particularly when considering longer timeframes.

3.2. Assessment of the viability and survival of culturable bacteria

The compaction dry density of bentonite inversely correlates with bacterial activity, primarily attributable to the reduced water activity (a$_w$). Investigations on MX-80 bentonite, compacted at 1.6 g cm^{-3}, indicated that an a$_w$ below 0.96 inhibited bacterial activity, leading to spore formation or bacterial dormancy (Stroes-Gascoyne et al., 2010). In our study, the initial dry density of 1.7 g cm^{-3} corresponded to an a$_w$ of 0.94–0.95, slightly below the threshold for suppressing bacterial activity. Therefore, the survival, viability and activity of specific bacterial groups has to be considered. The quantification of SRB within each treatment was determined by the Most Probable Number (MPN) method at 30 °C (one optimal growth temperature for SRB), and at 60 °C. Moreover, a molecular-level identification was conducted from the bacterial isolates, focusing on moderate-thermophilic bacteria able to grow at 60 °C and some anaerobic bacteria involved in the biogeochemical cycle of sulfur and iron.

3.2.1. Quantification of the most probable number of SRB

All bottles incubated at 60 °C, including negative controls (uninoculated Postgate media), exhibited the black precipitate that we would count as positive for SRB growth in the MPN enumeration. To check whether the precipitate was due to abiotic factors (e.g., high temperature) or to bacterial growth, selected dilutions from the different

treatments were plated on agar-Postgate dishes and incubated anaerobically at 60 °C. After 4 weeks of anaerobic incubation, no colonies were detected. Therefore, it was assumed that the presence of black precipitates in the bottles was mediated by unknown abiotic factors (e.g., reaction of some of the components of the medium to the high temperature of 60 °C).

However, the MPN enumeration showcased the viability and survival of culturable SRB across all treatments at 30 °C (Table 2). The values ranged between 9.5×10^1 and 2.5×10^3 MPN g^{-1} of bentonite (samples StB_1y and B.eD_1y, respectively). The growth detection of this group of bacteria showed their ability to survive despite the harsh incubation conditions within the bentonite blocks after one-year incubation (e.g., high dry-density compaction and temperature). Moreover, it was evidenced that SRB are even able to withstand the heat shock produced by the tyndallization process as shown in the StB_1y (9.5×10^1 MPN g^{-1} bentonite) and StB.eD_1y (1.5×10^2 MPN g^{-1} bentonite).

Following one-year incubation, the bentonite samples that were sterilized (StB_1y and StB.eD_1y) showed a decrease in the number of SRB compared to the preincubation bentonite (t. 0), while the unsterilized samples (B_1y and B.eD_1y) increased in SRB number (Table 2). Moreover, samples amended with electron donors/acceptor (B.eD_1y and StB.eD_1y) exhibited a slight increase compared to unamended samples (B_1y and StB_1y). Hence, it can be assumed that the tyndallization process had a slight long-term negative impact on the number of SRB, while the addition of acetate, lactate, and sulfate had a positive effect. Martinez-Moreno et al. (2023) demonstrated that the addition of electron donors/acceptor before (t. 0) and after one-year anaerobic incubation at 30 °C stimulated the number of SRB in highly compacted bentonite blocks. Additionally, in our study, a lower number of SRB was observed in the sterile samples (StB_1y and StB.eD_1y) after the incubation at 60 °C compared to those incubated at 30 °C. Moreover, the bentonite compaction at high density (1.7 g cm^{-3}) and the absence of a renewal water flow and/or organic compounds are adverse conditions making the bentonite blocks a hostile environment for the bacterial growth and viability over time. Previous studies have demonstrated that the increase in the density of the bentonite compaction has a negative effect on the viability of bacteria (e.g., SRB) (Bengtsson and Pedersen, 2017; Stroes-Gascoyne et al., 2006). Some SRB such as *Desulfosporosinus* and *Desulfotomaculum* could cope with harsh environments by spore formation, or by entering in a dormant state (desiccated cells) in dry bentonite (Grigoryan et al., 2018; Masurat et al., 2010). Groundwater infiltration into the repository could rewet and enrich the bentonite with organic matter, creating a less harsh environment for SRB. Consequently, it is important to know the ability of this group of bacteria to become active after periods of harshness within the DGR environment. Some studies have also observed the ability of SRB to withstand high temperatures (75–120 °C) and recover their cell viability after being enriched (Martinez-Moreno et al., 2023; Masurat et al., 2010). However, it should be noted that the MPN method provides approximate information about the number of SRB per gram of bentonite. Nonetheless, it is important to isolate and identify molecularly the bacteria of interest to further explore how incubation conditions affect their viability and potential long-term influence on DGR safety.

3.2.2. Isolation and molecular identification of moderate-thermophilic aerobic and anaerobic bacteria

Modified-Postgate agar medium was employed to isolate anaerobic bacteria from the positive bottles of the MPN experiment at 30 °C and 60 °C. In addition, oligotrophic culture medium R2A and 10 % LB were used to isolate microbial strains capable of withstanding and growing at 60 °C. No colonies were detected in agar-Postgate and R2A media incubated at 60 °C. As previously mentioned, the absence of colony formation on agar-Postgate incubated at 60 °C from the MPN bottles confirmed that this bacterial group was unable to exhibit activity at 60 °C. However, 9 pure cultures of anaerobic bacteria on modified Postgate were isolated at 30 °C. In addition, 13 pure cultures of aerobic bacteria were isolated on 10 % LB medium at 60 °C.

Four out of the 9 anaerobic bacterial colonies belonged to the genus *Anaerosolibacter* followed by *Pseudomonas*, *Sporacetigenium*, *Pelosinus*, and the order Clostridiales (Table 3). Among the 13 aerobic bacterial isolates, 10 strains belonged to the genus *Aeribacillus* (99.92 % identity related to *A. composti* N.8) and 3 belonged to the genus *Staphylococcus* (99.91 % identity related to *S. epidermidis* Fussel) (Table 3).

Regarding the strains isolated from the modified-Postgate medium, the closest phylogenetic relative for *Pseudomonas* was *P. lurida* EOO26. It was reported that this strain exhibited high metal tolerance, including Cu, and was associated to the anaerobic biocorrosion of steel-based metal canisters related to the DGR (Kumar et al., 2021; Jia et al., 2017). The strain Pg_2 belonged to the order Clostridiales, which encompass only strict anaerobic bacteria. The closest phylogenetic relative of this strain was the spore-forming *Clostridium thermarum* isolated from hot spring of Yunnan (China) presenting a temperature growth range of 28–50 °C (Liu et al., 2020). Another isolated strain was Pg_3, which was closely related to *Anaerosolibacter carboniphilus*, a strictly anaerobic, sulfate and iron-reducing bacterium that grows in a temperature range of 20–45 °C, and was previously isolated from coal contaminated soil of Republic of Korea (Hong et al., 2015). Regarding *Sporacetigenium*, although this bacterium has no sulfate-reducing capacity, it is also spore-forming and an obligate anaerobic bacterium with a growth range between 20 and 42 °C (Chen et al., 2006). Moreover, *S. mesophilum* is able to produce acetate, ethanol, hydrogen and carbon dioxide from glucose as major fermentation products that may be available for other microorganisms in the bacterial community of the bentonite. Finally, the closest phylogenetic strain for Pg_6 was *Pelosinus fermentans*. This is a spore-forming iron-reducing bacterium, able to use acetate and lactate as carbon sources and grow between 4 and 36 °C (Shelobolina et al., 2007). Some of the strains isolated in this study using the agar modified-Postgate medium for SRB do not exhibit the ability to reduce sulfate based on the cited literature for each genus (Kumar et al., 2021; Jia et al., 2017; Liu et al., 2020; Chen et al., 2006; Chen et al., 2006). The growth ability of these strains in the agar modified-Postgate may be associated with the capability of use some reagent from the medium but without using the sulfate as electron acceptor.

Aeribacillus composti is an obligate aerobic, spore-forming bacterium

Table 3
Affiliation of the 16S rRNA gene sequences of the isolates. RDP Classifier shows taxa (G: genera/O: order) and ID with a 100 % of confidence threshold (C.T.) based on a naive Bayesian classifier providing an accurate taxonomic placement of rRNA gene sequences. BLAST shows the closet phylogenetic relative strain, their percentage of identity and the accession number.

Isolate	Medium	Incubation	RDP Classifier	BLAST		
			Taxa 100 % C.T.	Closet Phyl. Relative	Ident. (%)	Accession no.
B.eD_8	LB	Aerob./60 °C	G_Aeribacillus	*A. composti* N.8	99.92	NR_159152.1
B.eD_1	LB	Aerob./60 °C	G_Staphylococcus	*S. epidermidis* Fussel	99.91	NR_036904.1
Pg_1	Postgate	Anaerob./30 °C	G_Pseudomonas	*P. lurida* P513/18	99.71	NR_042199.1
Pg_2	Postgate	Anaerob./30 °C	O_Clostridiales	*C. thermarum* GA15002	98.13	NR_178823.1
Pg_3	Postgate	Anaerob./30 °C	G_Anaerosolibacter	*A. carboniphilus* IRF19	99.72	NR_178620.1
Pg_5	Postgate	Anaerob./30 °C	G_Sporacetigenium	*S. mesophilum* ZLJ115	99.50	NR_043101.1
Pg_6	Postgate	Anaerob./30 °C	G_Pelosinus	*P. fermentans* DSM 17108 R7	98.95	NR_043577.1

isolated from olive mill pomace compost that grows in a temperature range between 50 and 65 °C (Finore et al., 2017). Moreover, *Staphylococcus epidermidis* is a commensal bacterium of human skin that may be an opportunistic microorganism. Strains belonging to this facultative anaerobe have been isolated in hostile environments such as hot springs in Taporan area (India), showing growth capacity at temperatures between 20 °C–70 °C (Pandey et al., 2015). The presence of *Staphylococcus* in the bentonite samples could be related to anthropogenic activities in the El Cortijo de Archidona's sampling site. The presence and survival of these aerobic bacteria could be related to the presence of oxygen molecules trapped in the bentonite before or during the compaction process (Burzan et al., 2022; Stroes-Gascoyne et al., 2010).

These findings clearly demonstrated that the isolated strains exhibited the capability to tolerate elevated temperatures (moderate-thermophilic bacteria), as well as specific metals such as copper. They are also actively participating in processes related to acetate and lactate consumption/production. Moreover, their capacity to be involved in iron and sulfate reduction was of particular significance. The isolation and taxonomic identification of bacteria form the studied samples are crucial for determining their potential impact on the materials' alteration within the DGR, especially their role in influencing the corrosion of future metal canisters.

3.3. Microbial diversity responses to incubation conditions

Samples before (t. 0) and after one year of anaerobic incubation at 60 °C were subjected to DNA extraction in triplicate. Despite multiple attempts, none of the three replicates of unamended samples (electron donors/acceptor free samples) incubated at 60 °C for one year under anaerobic conditions (B_1y and StB_1y) yielded enough DNA of satisfactory quality for sequencing. The use of highly compacted bentonite blocks (1.7 g cm^3 dry density), along with its low permeability, high swelling capacity, and incubation conditions (anaerobiosis and high temperature), created a harsh environment for the presence and survival of indigenous bacteria (Martinez-Moreno et al., 2023). These extreme conditions could affect and decrease drastically the yield of the DNA extracted due to the possible low number of bacterial cells in the samples (Povedano-Priego et al., 2021). As previously mentioned, electron donors and sulfate were added to stimulate indigenous bacteria (Matschiavelli et al., 2019; Grigoryan et al., 2018), thereby enhancing DNA extraction post-incubation. Accordingly, this section will focus on analyzing the impact of temperature (60 °C), compaction density (1.7 g cm^{-3}), and sterilization (tyndallization) on the microbial community within the amended compacted bentonite under anoxic conditions after one year incubation (B.eD, StB.eD, B.eD_1y, StB.eD_1y).

For these samples, enough sequencing depth was achieved as shown by the rarefaction curves (Supplementary Fig. S1). The sequence reads ranged from 2868 to 431,964. Some replicates were not included in this study because of a failure in the library preparation or sequencing step (B.eD_1y_R3, StB.eD_R3, and StB.eD_1y_R1). Alpha-diversity indices of the treatments are shown in Table 4 (Supplementary Table S2 for individual samples). After one-year incubation, a drastic decrease in the Richness values (Sobs and Chao1) of both bentonite (B.eD_1y) and sterile bentonite (StB.eD_1y) samples was evidenced. Furthermore, it

was notable that this reduction in richness was more pronounced in the sterilized bentonite sample (StB.eD_1y). The diversity indices (ShannonH and SimpsonD) followed the same pattern. Pre-incubation samples (B.eD and StB.eD) indicated high diversity (>3 and close to 1, respectively), while after-incubation samples (B.eD_1y and StB.eD_1y) showed low values (<3 and far from 1, respectively) indicating taxa dominance.

As a result of amplifying V3-V4 variable regions of 16S rRNA gene, a total of 779 OTUs were identified (Supplementary Data S1) and classified into 32 different phyla (Supplementary Table S3). Among these, 2 phyla were attributed to the Archaea domain (representing 0.01 % of the total relative abundance), while the remaining 30 were associated to 29 Bacteria domain (99.99 % of the total) and 1 OTU was unassigned. The most dominant phyla were Actinobacteriota (47.52 %) and Proteobacteria (37.62 %), followed by Chloroflexi (5.19 %), Firmicutes (3.68 %), Gemmatimonadota (1.38 %), and Acidobacteriota (1.26 %).

Principal coordinate analysis (PCoA) at genus level, using Bray-Curtis distance, revealed the dissimilarity of microbial communities between different treatments (Fig. 2). A distinct separation was evidenced between the samples after (B.eD_1y and StB.eD_1y) and before (B.eD and StB.eD) incubation. Moreover, the samples prior to incubation showed a division into two different clusters: bentonite (B.eD) and sterile bentonite (StB.eD). Moreover, no dissimilarities were found between the samples after the incubation, irrespective of whether the bentonite was sterilized or not (B.eD_1y and StB.eD_1y). PCoA suggested that the bentonite tyndallization affected the microbial diversity before incubation. However, this conditioning factor is not observed after one year of anaerobic incubation at 60 °C.

In general, the most representative OTUs were *Pseudomonas*, *Nocardioides*, and unclassified Micrococcaceae (23.00 %, 14.67 %, and 8.40 %, respectively), followed by Chloroflexi Gitt-GS-136, *Promicromospora*, *Marmoricola*, and unclassified Nocardioidaceae (3.22 %, 2.39 %, 2.13 %, and 2.12 %, respectively) (Fig. 3, Supplementary Data S1). In the pre-incubation samples (B.eD and StB.eD), the prevailing OTUs were *Nocardioides* (27.23 % and 11.92 %), unclassified *Micrococcaceae* (15.04 % and 6.23 %), and Chloroflexi Gitt-GS-136 (2.74 % and 6.42 %), which exhibited a substantial reduction in their relative abundance after the incubation, even disappearing (0.03 % and 0.00 %; 1.78 % and 0.70 %; 0.08 % and 0.00 %; respectively) (Fig. 3 and Supplementary Data S1). However, in the post-incubation samples (B.eD_1y and StB.eD_1y), the taxa dominance observed in the alpha-diversity
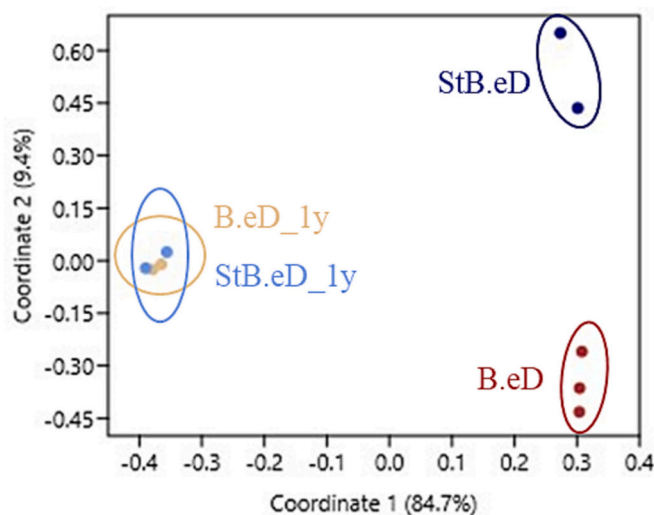
Table 4
Richness (Sobs/Chao1), diversity (ShannonH. and SimpsonD), and evenness (ShannonE) indices. Glossary: B: bentonite; StB: sterilized bentonite; eD: addition of acetate, lactate, and sulfate; 1y: after one year of anaerobic incubation at 60 °C.

	Sobs/Chao1	ShannonH	SimpsonD	ShannonE
B.eD	523	5.04	0.89	0.56
B.eD_1y	198	1.41	0.27	0.17
StB.eD	582	6.60	0.97	0.72
StB.eD_1y	126	2.12	0.47	0.30

Fig. 2. Principal Coordinate Analysis (PCoA) plot revealing the dissimilarity of microbial genera communities of the bentonite samples in duplicates (triplicates in B.eD). Distance based on Bray-Curtis. Glossary: B: bentonite, StB: sterilized bentonite, eD: addition of acetate, sulfate, and lactate; 1y: after one year of anaerobic incubation at 60 °C.
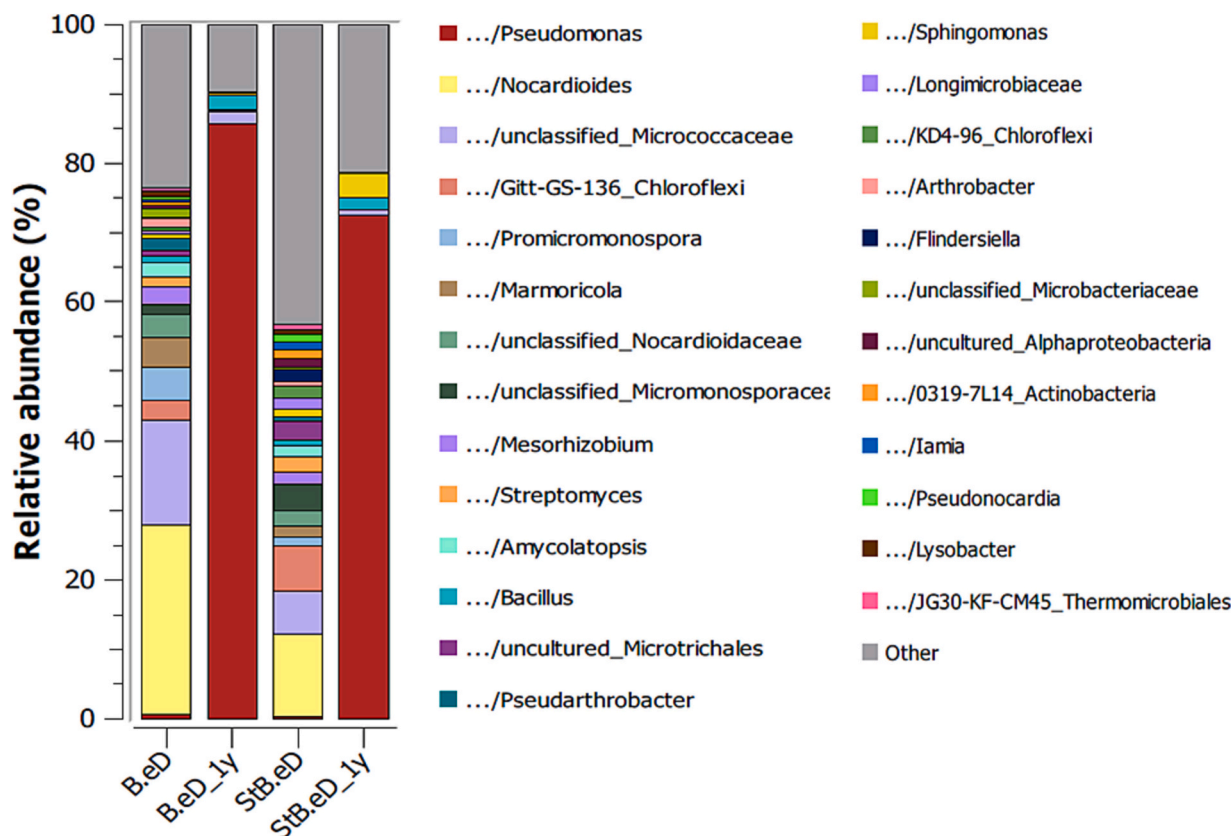
Fig. 3. OTU relative abundance (%) of the bacterial and archaeal communities of the bentonite samples in duplicates (triplicate in B.eD). Bar plot representing a cut off ≥0.50 %. Glossary: B: bentonite, StB: sterilized bentonite, eD: addition of acetate, sulfate, and lactate; 1y: after one year of anaerobic incubation at 60 °C.

values (Table 4) corresponded to an evident increase (Δ) in the relative abundance of the genus *Pseudomonas* with respect to the pre-incubation samples (Δ 84.92 % in B.eD_1y, and Δ 72.23 % in StB.eD_1y).

Previous research conducted at 30 °C, demonstrated that microbial communities exhibited only slight changes after one year of anaerobic incubation (Martinez-Moreno et al., 2023). In contrast, the present study revealed that the incubation temperature of 60 °C seems to be a clear limiting factor, reducing the microbial diversity of the bentonite and resulting in the predominance of the genus *Pseudomonas* in the samples. This is a facultative anaerobe bacterium that may use acetate and lactate as electron donor under anaerobic conditions (Chen et al., 2020; Essén et al., 2007; Eschbach et al., 2004). The experimental conditions of this study, i.e., high compaction and dry density, anaerobic conditions, and 60 °C incubation temperature, greatly restrict the potential presence and activity of bacteria. In situations of limited energy and physicochemical stress, microorganisms might significantly reduce their size and morphological characteristics to enhance their survival. Species of the genus *Pseudomonas* such as *P. syringae* have been demonstrated to decrease their size under harsh conditions (Monier and Lindow, 2003). Furthermore, previous research reported on the capacity of *Pseudomonas* spp. to be involved in the corrosion of carbon steel and copper materials within the context of DGR, through the reduction of iron and nitrates, respectively (Shrestha et al., 2022; Jia et al., 2017; Dou et al., 2022).

Next to *Pseudomonas* (85.62 % and 72.55 %), the dominant taxa in the post-incubation samples (B.eD_1y and StB.eD_1y), were *Bacillus* (2.01 % and 1.74 %, respectively), unclassified Micrococcaceae (1.78 % and 0.70 %, respectively), *Anaerosolibacter* (1.06 % and 1.50 %), and *Sphingomonas* (0.21 % and 3.55 %). The genus *Bacillus* encompasses a broad number of species known for their remarkable resistance and adaptability to a wide range of extreme environmental conditions (e.g., formation of endospores, metabolic versatility or cellular protection strategies). Hence, the occurrence in the post-incubation samples could

be attributed to the aforementioned mechanisms. Moreover, *Anaerosolibacter* is an obligate anaerobe, mesophilic bacterium, able to use Fe (III), elemental sulfur, thiosulfate and sulfate as electron acceptors and demonstrated the capability to tolerate temperatures reaching up to 45 °C (Hong et al., 2015). Regarding *Sphingomonas*, this genus can assimilate lactate and acetate (Vaïtilingom et al., 2010). Interestingly, certain strains within *Sphingomonas* have been found to play a role in the sulfur biogeochemical cycle through a process known as biodesulfurization, which involves the removal of sulfur from various materials. They were also reported to be implicated in the MIC of copper cold-water pipes (Cui et al., 2016; White et al., 1996).

In this study, SRB were detected in the samples B.eD, B.eD_1y, and StB.eD, represented by the phylum Desulfobacterota with low relative abundances (0.01 %, 0.02 %, and 0.03 % in total, respectively) (Supplementary Table S3). Moreover, genera such as *Desulfosporosinus*, *Desulfotomaculum*, *Pelosinus*, and *Sporacetigenium* were detected in a very low relative abundance in samples B.eD_1y, StB.eD and StB.eD_1y (≤0.03 %), being *Anaerosolibacter* more represented in sample B.eD_1y and StB.eD_1y (1.06 % and 1.50 %, respectively) (Supplementary Data S1). Despite the limited occurrence of this bacterial group in the samples, delving into their study remains crucial due to their important role in the long-term anaerobic corrosion of copper canisters within the DGR context (Bengtsson and Pedersen, 2017).

3.4. Surface characterization of copper disks

The main corrosive agent of copper under DGR relevant conditions will be biogenic hydrogen sulfide generated by SRB (Bengtsson and Pedersen, 2017). Under anaerobic conditions, these bacteria have the ability to oxidize lactate (as an electron donor) while simultaneously reducing sulfate as terminal electron acceptor (Thauer et al., 2007). This process yields HS$^-$ as a metabolic product, which may subsequently
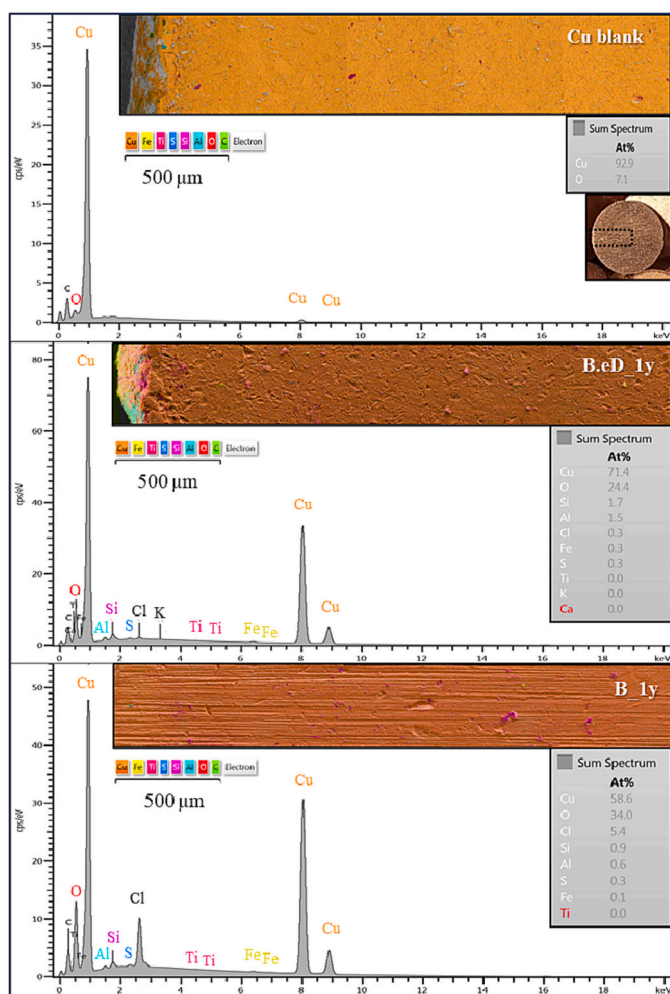
Fig. 4. Sum EXD spectrum associated with elemental quantification of VP-FESEM five-micrographs composition from a selected area (edge to center) of Cu disks blank, and from samples B.eD_1y and B_1y.

combine with H^+ to generate H_2S. The H_2S released by SRB can dissociate into H^+ and HS^-. The latter can migrate to the surface of the copper and react with the metal, resulting in the formation of Cu_2S (Dou et al., 2020). Chen et al. (2014) demonstrated that in anaerobic environments, SRB possess the capability to attach to copper surfaces, forming a biofilm, and generating Cu_2S as the main corrosion product. The generation of extracellular polymeric substances (EPS) from the SRB biofilm, and subsequently from the Cu_2S film, serves to diminish copper's toxicity for SRB.

In our study, VP-FESEM analyses were conducted on Cu disks taken from the blocks from each treatment after one-year incubation. Fig. 4 shows a composition of five adjacent areas of approximately 560×430 µm each selected from the edge to the center of the disk. The resulting five-images composition from Cu blank (copper disk before experimental setup), previously characterized in Martinez-Moreno et al. (2023), B.eD_1y, and B_1y samples revealed the surface distribution of Cu, Fe, Ti, S, Si, Al, O, and C, and the general EDX and quantification of these elements in the study area as a sum of the EDX spectra in >10 selected points in each disk. Microscopy images from the sterilized bentonite treatments are not shown since no alterations or differences were observed with respect to the samples in Fig. 4.

The metal surfaces seemed to be nearly unaltered. However, certain irregularities on the surface were detected, potentially resulting from the pressure applied by fractions of the bentonite during the compaction process of the blocks' assembly. Residual bentonite presented on the

copper surface was observed, shown as pink and yellow areas in Fig. 4, and corresponding to the presence of Si, Fe, Ti, and Al in the EDX spectrum. According to the sum spectrum in Fig. 4, the presence of S was very low in the studied areas in both B.eD_1y and B_1y samples. No copper sulfide (Cu_xS) precipitates were observed.

Complementarily, to assess and compare the surface compositions of each copper disks, XPS was employed. Wide scans revealed the presence of Cu, C, O, Si, Na, Fe, Mg and Al on the surface of the samples. Excluding Cu, these elements were likely due to bentonite adhered to the surface of the disks. High resolution scans for the Cu 2p region displayed elemental copper peaks on all samples and also revealed the probable existence of CuO. Fig. 5 shows the high resolution scans for the Cu 2p region on samples B_1y and B.eD_1y. Two sharp peaks, corresponding to Cu $2p_{3/2}$ and Cu $2p_{1/2}$, were seen at 934.21 eV and 954.17 eV, respectively. These peaks are in accordance with previously reported data attributed to elemental copper (Wagner et al., 1979) and were evident on every sample. The high-resolution scan of this region also unveiled the presence of CuO on the surface of all samples (Fig. 5). The peaks observed at 943.49 eV and 962.89 eV, and the distance between Cu $2p_{1/2}$ and Cu $2p_{3/2}$ peaks (of 19.96 eV), presented clear evidence for the presence of CuO (Wagner et al., 1979). High resolution spectra of the Cu 2p region of untreated copper disks (blanks) did not show the presence of CuO (Supplementary Fig. S2). The presence of oxygen on the surface of the samples may be due to the high affinity of the copper for oxygen molecules. Some oxygen particles can remain trapped in the bentonite (Burzan et al., 2022) and could participate in the oxidation of copper.

As mentioned before, anaerobic MIC on copper surfaces should also reveal the presence of Cu_xS. Previous studies have shown that peaks for CuS are observed at approximately 932.2 eV in the high-resolution Cu 2p scans (Krylova and Andrulevičius, 2009). However, if this was present, it would have been overshadowed by the Cu $2p_{3/2}$ peak and therefore any presence of CuS could not be confirmed from the Cu 2p high resolution spectra. Therefore, in order to investigate further, high resolution scans on the S 2p region between 143 and 180 eV were conducted.

The XPS spectra in the S 2p region between 143 and 180 eV (Fig. 5) revealed a peak around 155.3 eV corresponding to Si 2s on all samples, due to bentonite adhered on the scanned area of the sample (Clarke and Rizkalla, 1976). In conjunction with the Si 2s peak, samples from different treatments showed the presence of sulfur on the surface in at least two different moieties: sulfate and sulfide. Sulfate was detected on all samples (Fig. 5 and Supplementary Fig. S3) with peaks at roughly 169 eV (Fantauzzi et al., 2015). However, sulfide was only detected on samples B.eD_1y and StB.eD_1y (Fig. 5 and Supplementary Fig. S3) with a very small peak around 163.5 eV. This binding energy has been previously observed for metal sulfides and disulfides, with reported values between 162.9 and 164.5 eV (Hussain et al., 2018). According to the literature, the binding energies reported for CuS and Cu_2S peaks are around 162.2 eV (Krylova and Andrulevičius, 2009; Scheer and Lewerenz, 1994), however, these signals were less evident from the acquired spectra.

Reflectance micro-FTIR spectroscopic analysis was employed to investigate the possible existence of microbial biofilm on the sample surfaces. The results obtained for samples B.eD_1y and B_1y are shown in Fig. 6. An optical microscope was used to inspect sections of the disks, while the infrared microscope was employed for scanning. False-color images were produced to reveal the location of IR-active functional groups. The absorbance scale on the left indicates the abundance of molecules absorbing the infrared radiation on a specific area, with regions with a greater concentration of organic or IR-active compounds depicted in red, and regions with low absorbance areas depicted in dark blue, indicating the absence of IR-absorbing functional groups. The regions lacking IR-absorbing molecules exhibited a generally flat spectrum, often corresponding with exposed copper areas observed on the disks (Fig. 6).

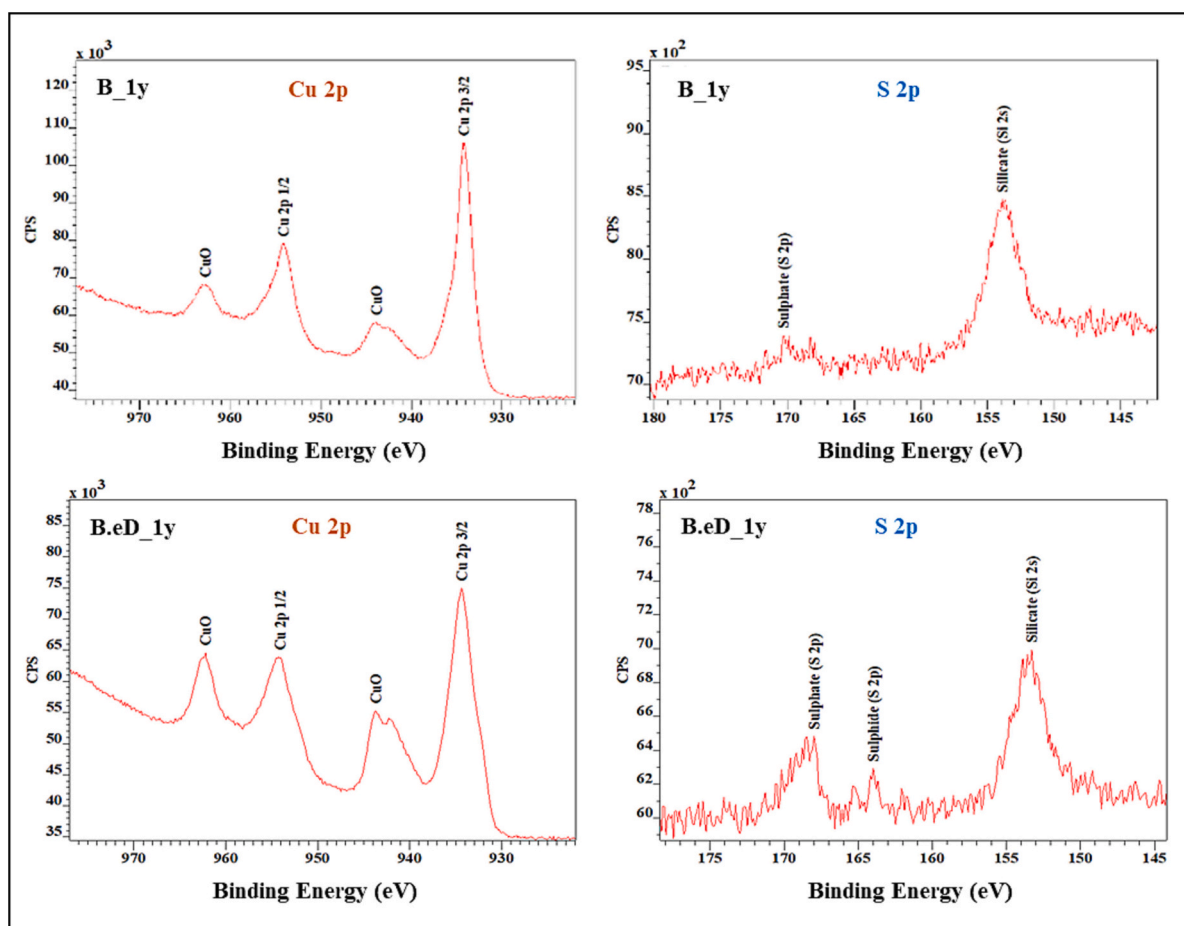The presence of proteins, lipids, and polysaccharides bands in a

Fig. 5. High resolution XPS spectra of: Cu 2p (region between 922 and 977 eV), left, and S 2p (region between 143 and 180 eV), right, for samples B_1y (top) and BeD_1y (bottom).

spectrum can normally be correlated to the presence of microbial macromolecules on the surface of the samples, within the detection limits of this technique. Remains of bentonite adhered to the disks surface were also identified on the samples. The spectra obtained from these areas displayed the characteristic spectral features of Si—O, Si—O—Si, Al—OH, and other inorganic compounds commonly associated with bentonite (blue spectra, Fig. 6). Bands for Al—OH bending vibrations are located at around 850 cm^{-1} (Bishop et al., 2002). Si—O and Si—O—Si stretching vibrations demonstrate bands at 1110 cm^{-1} and 980 cm^{-1}, respectively (Gaggiano et al., 2013). Bands associated with proteins, lipids, and polysaccharides were identified on samples B_1y and B. eD_1y, supporting the existence of organic substances typically linked with microbial cells or their metabolites (Fig. 6). The signals at approximately 1640 cm^{-1} and 1540 cm^{-1} were attributed to the amide I and II bands, respectively. Stretching of the carbon-oxygen double bonds (νC—O) was the primary contributor to the amide I band whereas a combination of bending N—H bonds (δN—H) and stretching C—N (νC—N) groups within amides were responsible for the amide II band. These spectral bands have been extensively reported in the literature for samples associated with bacteria (Jiang et al., 2004; Naumann et al., 1991; Ojeda and Dittrich, 2012; Orsini et al., 2000).

The detection of sulfur on the surface of copper disks could be related to bacterial activity (Pedersen, 2010). Martinez-Moreno et al. (2023) observed small sized precipitates of Cu$_x$S on the surface of copper disks incubated at 30 °C. In contrast, no precipitates were observed by microscopy in this study after one year of incubation at 60 °C. However, the sulfur was detected in the form of sulfate and sulfide. The presence of sulfate in the sample B.eD_1y could be related to the addition of this electron aceptor during the pretreatment of the bentonite, which was in direct contact with the copper disk during the incubation time. While SRB growth was not observed at 60 °C in the modified-Postgate medium, it is possible that some bacteria within this group could exhibit activity at this temperature.

A deep characterization of the copper surface was performed in this study. The microorganism's infrared spectra were frequently found in close proximity to the bentonite, implying a potential association between these microorganisms and the bentonite rather than direct contact with the copper surface. The identification of sulfide further suggests the possibility of SRB activity, which could potentially influence the condition of the copper surface. However, it is essential to conduct additional investigations to substantiate this hypothesis since no precipitates related to the formation of Cu$_x$S were observed by microscopy.

4. Conclusions

The current study investigated the effect of physicochemical factors, including high temperature (60 °C), high dry-compaction density of bentonite, the addition of electron donors/acceptor, the pre-sterilization of bentonite, and anoxic conditions after one year, on the microbiology of highly compacted bentonite. It further explores the resulting impacts of the microbial communities on the mineralogical stability of the bentonite and the corrosion of copper materials related to the engineering barriers of future DGR of nuclear waste. The results show that no illitization of smectite was observed under different conditions, indicating the mineralogical stability of the bentonite and its key role as
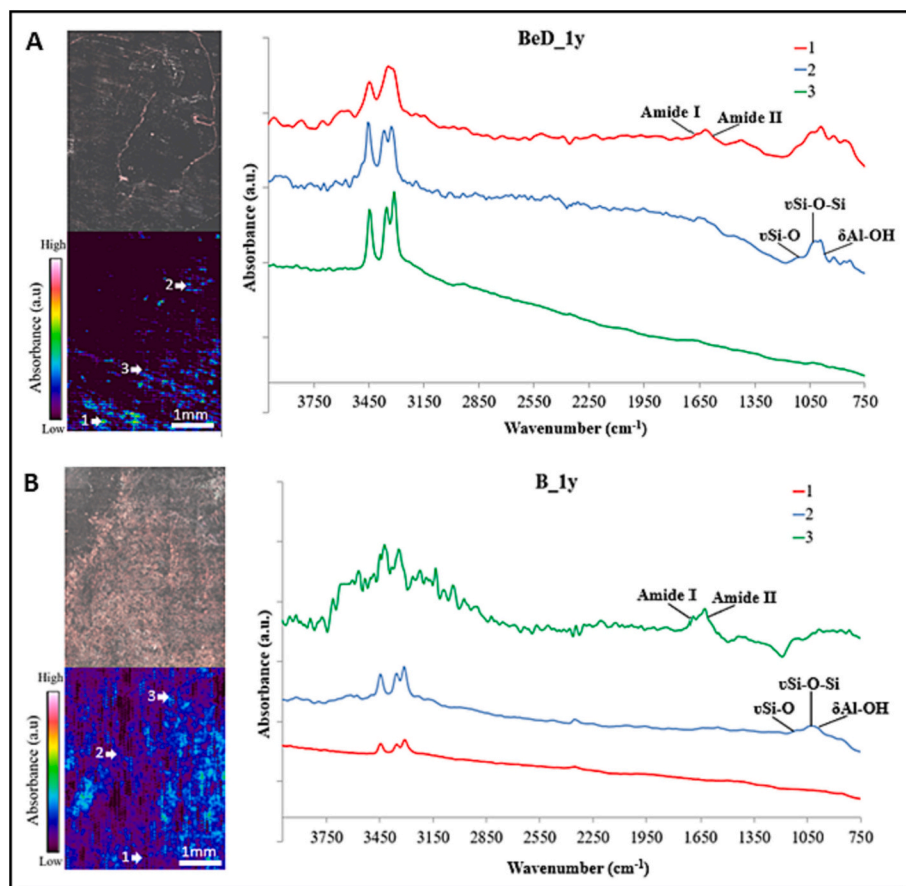
Fig. 6. Reflectance micro-FTIR spectroscopy from B.eD_1y (A) and B_1y (B) samples. Top left: optical image of the scanned region. Bottom left: false-color image of the sample scanned using reflectance micro-FTIR spectroscopy. Right: infrared spectra of 3 different regions on the sample.

effective barrier for future DGR. Our study demonstrated that the applied tyndallization procedure to sterilize the bentonite was not sufficient to eradicate SRB as viable species since showed growth after one year in amended and unamended samples with electron donors and acceptor. During the tyndallization, the temperature does not exceed 110 °C to prevent any alteration of the bentonite properties. This temperature could be not enough to destroy all the bacteria. Other hypothesis could be the effect of bentonite, which could protect some bacteria from the tyndallization heat-shock due to its role as buffer, but this needs more research. Moreover, in the non-sterilized samples, the addition of electron donors/acceptor was beneficial for the viability of SRB. Interestingly, we were able to isolate species with the ability to grow at 60 °C but only under aerobic conditions. For the anaerobic species, the conditions needed to be lowered to 30 °C to observe growth. Therefore, although they remain viable, these species are probably not highly active at 60 °C. This was further confirmed by the presence of sulfide, which indicated sulfate reduction, but not in sufficient amounts to observe visual changes on the surface of copper disks. Furthermore, the isolated strains were also observed in the sequencing results, which showed a decreased bacterial diversity after one year of anaerobic incubation with *Pseudomonas* becoming the dominant genus and, to a lesser extent, some bacterial groups adapted to extreme conditions.

These findings provide new perspectives on understanding the biogeochemical processes at the interface bentonite/Cu canister after repository closure. Specifically, this study provides new insights about how the gradual increase of temperature, due to the heat produced by the decay process of the waste, within the DGR could impact the microbial communities and, subsequently, affects the stability of the

bentonite and the copper-based metal canisters.

Supplementary data to this article can be found online at https://doi.org/10.1016/j.scitotenv.2024.170149.

CRediT authorship contribution statement

Marcos F. Martinez-Moreno: Writing – review & editing, Writing – original draft, Visualization, Validation, Methodology, Investigation, Formal analysis, Data curation, Conceptualization. **Cristina Povedano-Priego:** Writing – review & editing, Visualization, Validation, Methodology. **Adam D. Mumford:** Writing – review & editing, Writing – original draft, Validation, Investigation, Formal analysis, Data curation. **Mar Morales-Hidalgo:** Writing – review & editing, Methodology. **Kristel Mijnendonckx:** Writing – review & editing, Validation, Supervision,

Resources. **Fadwa Jroundi:** Writing – review & editing. **Jesus J. Ojeda:** Writing – review & editing, Writing – original draft, Validation, Supervision, Investigation, Formal analysis. **Mohamed L. Merroun:** Writing – review & editing, Visualization, Validation, Supervision, Resources, Project administration, Methodology, Funding acquisition, Conceptualization.

Declaration of competing interest

The authors declare that they have no known competing financial interests or personal relationships that could have appeared to influence the work reported in this paper.

Data availability

The nucleotide sequences and metagenomics' raw data of this study were submitted to the sequence read archive (SRA) at NCBI: BioProject accession number PRJNA1045398 and PRJNA1044717, respectively.

Acknowledgements

References

Anderson, T.F., 1951. Techniques for the preservation of three-dimensional structure in preparing specimens for the electron microscope. Trans. N.Y. Acad. Sci. 13, 130–134. https://doi.org/10.1111/j.2164-0947.1951.tb01007.x.

Bengtsson, A., Pedersen, K., 2016. Microbial sulphate-reducing activity over load pressure and density in water saturated boom clay. Appl. Clay Sci. 132, 542–551. https://doi.org/10.1016/j.clay.2016.08.002.

Bengtsson, A., Pedersen, K., 2017. Microbial sulphide-producing activity in water saturated Wyoming MX-80, Asha and Calcigel bentonites at wet densities from 1500 to 2000 kg m^{-3}. Appl. Clay Sci. 137, 203–212. https://doi.org/10.1016/j.clay.2016.12.024.

Bishop, J., Madejová, J., Komadel, P., Fröschl, H., 2002. The influence of structural Fe, Al and Mg on the infrared OH bands in spectra of dioctahedral smectites. Clay Miner. 37 (4), 607–616. https://doi.org/10.1180/0009855023740063.

Burzan, N., Lima, R.M., Frutschi, M., Janowczyk, A., Reddy, B., Rance, A., Diomidis, N., Bernier-Latmani, R., 2022. Growth and persistence of an aerobic microbial community in Wyoming bentonite MX-80 despite anoxic in situ conditions. Front. Microbiol. 13, 858324 (doi:10.3389%2Ffmicb.2022.858324).

Caporaso, J.G., Kuczynski, J., Stombaugh, J., Bittinger, K., Bushman, F.D., Costello, E.K., Fierer, N., Gonzalez Peña, A., Goodrich, J.K., Gordon, J.I., Huttley, G.A., Kelley, S.T., Knights, D., Koening, J.E., Ley, R.E., Lozupone, C.A., McDonald, D., Muegge, B.D., Pirrung, M., Reeder, J., Sevinsky, J.R., Turnbaugh, P.J., Walters, W.A., Widmann, J., Yatsuneko, T., Zaneveld, J., Knight, R., 2010. QIIME allows analysis of high-throughput community sequencing data. Nat. Methods 7, 335–336.

Chen, S., Song, L., Dong, X., 2006. *Sporacetigenium mesophilum* gen. nov., sp. nov., isolated from an anaerobic digester treating municipal solid waste and sewage. Int. J. Syst. Evol. Microbiol. 56 (4), 721–725. https://doi.org/10.1099/ijs.63686-0.

Chen, S., Wang, P., Zhang, D., 2014. Corrosion behavior of copper under biofilm of sulfate-reducing bacteria. Corros. Sci. 87, 407–415. https://doi.org/10.1016/j.corsci.2014.07.001.

Chen, Z., Jiang, Y., Chang, Z., Wang, J., Song, X., Huang, Z., Chen, S., Li, J., 2020. Denitrification characteristics and pathways of a facultative anaerobic denitrifying strain, *Pseudomonas denitrificans* G1. J. Biosci. Bioeng. 129 (6), 715–722. https://doi.org/10.1016/j.jbiosc.2019.12.011.

Clarke, T.A., Rizkalla, E.N., 1976. X-ray photoelectron spectroscopy of some silicates. Chem. Phys. Lett. 37, 523–526. https://doi.org/10.1016/0009-2614(76)85029-4.

Cui, X., Zhao, S., Wang, B., 2016. Microbial desulfurization for ground tire rubber by mixed consortium-*Sphingomonas* sp. and *Gordonia* sp. Polym. Degrad. Stab. 128, 165–171. https://doi.org/10.1016/j.polymdegradstab. 2016.03.011.

Dou, W., Pu, Y., Han, X., Song, Y., Chen, S., Gu, T., 2020. Corrosion of Cu by a sulfate reducing bacterium in anaerobic vials with different headspace volumes. Bioelectrochemistry 133, 107478. https://doi.org/10.1016/j.bioelechem.2020.107478.

Dou, W., Pu, Y., Gu, T., Chen, S., Chen, Z., Xu, Z., 2022. Biocorrosion of copper by nitrate reducing *Pseudomonas aeruginosa* with varied headspace volume. Int. Biodeterior. Biodegradation 171, 105405. https://doi.org/10.1016/j.ibiod.2022.105405.

Eschbach, M., Schreiber, K., Trunk, K., Buer, J., Jahn, D., Schobert, M., 2004. Long-term anaerobic survival of the opportunistic pathogen *Pseudomonas aeruginosa* via pyruvate fermentation. J. Bacteriol. 186 (14), 4596–4604. https://doi.org/10.1128/jb.186.14.4596-4604.2004.

Essén, S.A., Johnsson, A., Bylund, D., Pedersen, K., Lundström, U.S., 2007. Siderophore production by *Pseudomonas stutzeri* under aerobic and anaerobic conditions. Appl. Environ. Microbiol. 73 (18), 5857–5864. https://doi.org/10.1128/AEM.00072-07.

Fairley, N.CasaX.P.S., 2.3.22 ed.; Casa Software Ltd.: 2019.

Fantauzzi, M., Elsener, B., Atzei, D., Rigoldi, A., Rossi, A., 2015. Exploiting XPS for the identification of sulfides and polysulfides. RSC Adv. 5 (93), 75953–75963. https://doi.org/10.1039/C5RA14915K.

Fernández, A.M., 2004. Caracterización y modelización del agua intersticial de materiales arcillosos: Estudio de la bentonita de Cortijo de Archidona. PhD Thesis. Editorial Ciemat. (ISBN84-7834-479-9, 505–pp.).

Fernández, A.M., Marco, J.F., Nieto, P., León, F.J., Robredo, L.M., Clavero, M.Á., Cardona, A.I., Fernández, S., Svensson, D., Sellin, P., 2022. Characterization of bentonites from the in situ ABM5 heater experiment at Äspö Hard Rock Laboratory, Sweden. Minerals 12 (4), 471. https://doi.org/10.3390/min12040471.

Finore, I., Gioiello, A., Leone, L., Orlando, P., Romano, I., Nicolaus, B., Poli, A., 2017. *Aeribacillus composti* sp. nov., a thermophilic bacillus isolated from olive mill pomace compost. Int. J. Syst. Evol. Microbiol. 67 (11), 4830–4835. https://doi.org/10.1099/ijsem.0.002391.

Gaggiano, R., De Graeve, I., Mol, J.M.C., Verbeken, K., Kestens, L.A.I., Terryn, H., 2013. An infrared spectroscopic study of sodium silicate adsorption on porous anodic alumina. Surf. Interface Anal. 45, 1098–1104. https://doi.org/10.1002/sia.5230.

García-Romero, E., María Manchado, E., Suárez, M., García-Rivas, J., 2019. Spanish bentonites: a review and new data on their geology, mineralogy, and crystal chemistry. Fortschr. Miner. 9, 696. https://doi.org/10.3390/min9110696.

Grigoryan, A.A., Jalique, D.R., Medihala, P., Stroes-Gascoyne, S., Wolfaardt, G.M., McKelvie, J., Korber, D.R., 2018. Bacterial diversity and production of sulfide in microcosms containing uncompacted bentonites. Heliyon 4, e00722. https://doi.org/10.1016/j.heliyon.2018.e00722.

Hall, D.S., Behazin, M., Binns, W.J., Keech, P.G., 2021. An evaluation of corrosion processes affecting copper-coated nuclear waste containers in a deep geological repository. Prog. Mater. Sci. 118, 100766 https://doi.org/10.1016/j.pmatsci.2020.100766.

Hammer, Ø., Harper, D.A., 2001. Past: paleontological statistics software package for educaton and data anlysis. Palaeontol. Electron. 4 (1), 1.

Hong, H., Kim, S.J., Min, U.G., Lee, Y.J., Kim, S.G., Roh, S.W., Kim, J.G., Na, J.G., Rhee, S.K., 2015. *Anaerosolibacter carboniphilus* gen. nov., sp. nov., a strictly anaerobic iron-reducing bacterium isolated from coal-contaminated soil. Int. J. Syst. Evol. Microbiol. 65 (Pt_5), 1480–1485. https://doi.org/10.1099/ijs.0.000124.

Huertas, F., Fariña, P., Farias, J., García-Siñeriz, J.L., Villar, M.V., Fernández, A.M., Martin, P.L., Elorza, F.J., Gens, A., Sánchez, M., Lloret, A., Samper, J., Martínez, M.Á., 2021. Full-scale engineered barriers experiment. Updated Final Report 1994–2004.

Hussain, S., Lalla, N.P., Kuo, Y.K., Lakhani, A., Sathe, V.G., Deshpande, U., Okram, G.S., 2018. Thermoelectric properties of Ag-doped CuS nanocomposites synthesized by a facile polyol method. Phys. Chem. Chem. Phys. 20, 5926–5935. https://doi.org/10.1039/C7CP07986A.

Jia, R., Yang, D., Xu, D., Gu, T., 2017. Anaerobic corrosion of 304 stainless steel caused by the *Pseudomonas aeruginosa* biofilm. Front. Microbiol. 8, 2335. https://doi.org/10.3389/fmicb.2017.02335.

Jiang, W., Saxena, A., Song, S., Ward, B.B., Beveridge, T.J., Myneni, S.C.B., 2004. Elucidation of functional groups on gram-positive and gram-negative bacterial surfaces using infrared spectroscopy. Langmuir 20, 11433–11442. https://doi.org/10.1021/la049043.

Kaufhold, S., Dohrmann, R., 2010. Stability of bentonites in salt solutions: II. Potassium chloride solution — initial step of illitization? Appl. Clay Sci. 49, 98–107. https://doi.org/10.1016/j.clay.2010.04.009.

Keech, P.G., Vo, P., Ramamurthy, S., Chen, J., Jacklin, R., Shoesmith, D.W., 2014. Design and development of copper coatings for long term storage of used nuclear fuel. Corros. Eng. Sci. Technol. 49 (6), 425–430. https://doi.org/10.1179/1743278214Y.0000000206.

Kim, J., Dong, H., Yang, K., Park, H., Elliott, W.C., Spivack, A., Heuer, V.B., 2019. Naturally occurring, microbially induced smectite-to-illite reaction. Geol. Soc. Am. Bull. 47, 535–539.

King, F., Hall, D.S., Keech, P.G., 2017. Nature of the near-field environment in a deep geological repository and the implications for the corrosion behaviour of the container. Corros. Eng. Sci. Technol. 52 (sup1), 25–30. https://doi.org/10.1080/1478422X.2017.1330736.

Krylova, V., Andrulevičius, M., 2009. Optical, XPS and XRD studies of semiconducting copper sulfide layers on a polyamide film. Int. J. Photoenergy. https://doi.org/10.1155/2009/304308.

Kumar, A., Voropaeva, O., Maleva, M., Panikovskaya, K., Borisova, G., Rajkumar, M., Bruno, L.B., 2021. Bioaugmentation with copper tolerant endophyte *Pseudomonas lurida* strain EOO26 for improved plant growth and copper phytoremediation by *Helianthus annuus*. Chemosphere 266, 128983. https://doi.org/10.1016/j.chemosphere.2020.128983.

Liu, D., Dong, H., Bishop, M.E., Zhang, J., Wang, H., Xie, S., Wang, S., Huang, L., Eberl, D.D., 2012. Microbial reduction of structural iron in interstratified illite-smectite minerals by a sulfate-reducing bacterium. Geobiology 10, 150–162. https://doi.org/10.1111/j.1472-4669.2011.00307.x.

Liu, L., Jiao, J.Y., Fang, B.Z., Lv, A.P., Ming, Y.Z., Li, M.M., Salam, N., Li, W.J., 2020. Isolation of *Clostridium* from Yunnan-Tibet hot springs and description of *Clostridium thermarum* sp. nov. with lignocellulosic ethanol production. Syst. Appl. Microbiol. 43 (5), 126104 https://doi.org/10.1016/j.syapm.2020.126104.

Lopez-Fernandez, M., Fernández-Sanfrancisco, O., Moreno-García, A., Martín-Sánchez, I., Sánchez-Castro, I., Merroun, M.L., 2014. Microbial communities in bentonite formations and their interactions with uranium. Appl. Geochem. 49, 77–86. https://doi.org/10.1016/j.apgeochem.2014.06.022.

Lopez-Fernandez, M., Cherkouk, A., Vílchez-Vargas, R., Jauregui, R., Pieper, D., Boon, N., Sanchez-Castro, I., Merroun, M.L., 2015. Bacterial diversity in bentonites, engineered barrier for deep geological disposal of radioactive wastes. Microb. Ecol. 70, 922–935. https://doi.org/10.1007/s00248-015-0630-7.

Madina, V., Insausti, M., Azkarate, I., Garmendia, I., Cuñado, M.A., 2005. Corrosion behaviour of container candidate materials for HLW disposal in granite-bentonite media. Afinidad 62 (519), 383–387.

Martinez-Moreno, M.F., Povedano-Priego, C., Morales-Hidalgo, M., Mumford, A.D., Ojeda, J.J., Jroundi, F., Merroun, M.L., 2023. Impact of compacted bentonite microbial community on the clay mineralogy and copper canister corrosion: a multidiskiplinary approach in view of a safe Deep Geological Repository of nuclear wastes. J. Hazard. Mater., 131940 https://doi.org/10.1016/j.jhazmat.2023.131940.

Masurat, P., Eriksson, S., Pedersen, K., 2010. Evidence of indigenous sulphate-reducing bacteria in commercial Wyoming bentonite MX-80. Appl. Clay Sci. 47, 51–57. https://doi.org/10.1016/j.clay.2008.07.002.

Matschiavelli, N., Kluge, S., Podlech, C., Standhaft, D., Grathoff, G., Ikeda-Ohno, A., Warr, L.N., Chukharkina, A., Arnold, T., Cherkouk, A., 2019. The year-long development of microorganisms in uncompacted bavarian bentonite slurries at 30 and 60 °C. Environ. Sci. Technol. 2019 (53), 10514–10524. https://doi.org/10.1021/acs.est.9b02670.

Meleshyn, A., 2011. Microbial processes relevant for long-term performance of radioactive waste repositories in clays. In: GRS-291. ISBN 978-3-939355-67-0. Available from: https://www.grs.de/sites/default/files/pdf/GRS-291.pdf.

Miller, J.H., 1972. Experiments in Molecular Genetics. Cold Spring Harbor.

Monier, J.M., Lindow, S.E., 2003. *Pseudomonas syringae* responds to the environment on leaves by cell size reduction. Phytopathology 93 (10), 1209–1216. https://doi.org/10.1094/PHYTO.2003.93.10.1209.

Naumann, D., Helm, D., Labischinski, H., 1991. Microbiological characterizations by FT-IR spectroscopy. Nature 351, 81–82. https://doi.org/10.1038/351081a0.

Ohazuruike, L., Lee, K.J., 2023. A comprehensive review on clay swelling and illitization of smectite in natural subsurface formations and engineered barrier systems. Nucl. Eng. Technol. 55, 1495–1506. https://doi.org/10.1016/j.net.2023.01.007.

Ojeda, J.J., Dittrich, M., 2012. Fourier transform infrared spectroscopy for molecular analysis of microbial cells. J. Microbiol. Methods 187–211. https://doi.org/10.1007/978-1-61779-827-6_8.

Ojovan, M.I., Steinmetz, H.J., 2022. Approaches to disposal of nuclear waste. Energies 15, 7804. https://doi.org/10.3390/en15207804.

Orsini, F., Ami, D., Villa, A.M., Sala, G., Bellotti, M.G., Doglia, S.M., 2000. FT-IR microspectroscopy for microbiological studies. J. Microbiol. Meth. 42, 17. https://doi.org/10.1016/S0167-7012(00)00168-8.

Pandey, A., Dhakar, K., Sharma, A., Priti, P., Sati, P., Kumar, B., 2015. Thermophilic bacteria that tolerate a wide temperature and pH range colonize the Soldhar (95 C) and Ringigad (80 C) hot springs of Uttarakhand, India. Ann. Microbiol. 65 (2), 809–816. https://doi.org/10.1007/s13213-014-0921-0.

Payer, J.H., Finsterle, S., Apps, J.A., Muller, R.A., 2019. Corrosion performance of engineered barrier system in deep horizontal drillholes. Energies 12, 1491. https://doi.org/10.3390/en12081491.

Pedersen, K., 2010. Analysis of copper corrosion in compacted bentonite clay as a function of clay density and growth conditions for sulfate-reducing bacteria. J. Appl. Microbiol. 108, 1094–1104. https://doi.org/10.1111/j.1365-2672.2009.04629.x.

Pentráková, L., Su, K., Pentrák, M., Stucki, J.W., 2013. A review of microbial redox interactions with structural Fe in clay minerals. Clay Miner. 48, 543–560. https://doi.org/10.1180/claymin.2013.048.3.10.

Povedano-Priego, C., Jroundi, F., Lopez-Fernandez, M., Sánchez-Castro, I., Martin-Sánchez, I., Huertas, F.J., Merroun, M.L., 2019. Shifts in bentonite bacterial community and mineralogy in response to uranium and glycerol-2-phosphate exposure. Sci. Total Environ. 692, 219–232. https://doi.org/10.1016/j.scitotenv.2019.07.228.

Povedano-Priego, C., Jroundi, F., Lopez-Fernandez, M., Shrestha, R., Spanek, R., Martín-Sánchez, I., Villar, M.V., Ševcǔ, A., Dopson, M., Merroun, M.L., 2021. Deciphering indigenous bacteria in compacted bentonite through a novel and efficient DNA extraction method: insights into biogeochemical processes within the deep geological disposal of nuclear waste concept. J. Hazard. Mater. 408, 124600 https://doi.org/10.1016/j.jhazmat.2020.124600.

Reasoner, D.J., Geldreich, E., 1985. A new medium for the enumeration and subculture of bacteria from potable water. Appl. Environ. Microbiol. 49, 1–7.

Robertson, C.E., Harris, J.K., Wagner, B.D., Granger, D., Browne, K., Tatem, B., Feazel, L.M., Park, K., Pace, N.R., Frank, D.N., 2013. Explicet: graphical user interface software for metadata-driven management, analysis and visualization of microbiome data. Bioinformatics 29, 3100–3101. https://doi.org/10.1093/bioinformatics/btt526.

Scheer, R., Lewerenz, H.J., 1994. Photoemission study of evaporated CuInS2 thin films. II. Electronic surface structure. J. Vac. Sci. Technol. A: Vac. Surf. Films. 12, 56–60. https://doi.org/10.1116/1.578858.

Shelobolina, E.S., VanPraagh, C.G., Lovley, D.R., 2003. Use of ferric and ferrous iron containing minerals for respiration by Desulfitobacterium frappieri. Geomicrobiol J. 20, 143–156. https://doi.org/10.1080/01490450303884.

Shelobolina, E.S., Nevin, K.P., Blakeney-Hayward, J.D., Johnsen, C.V., Plaia, T.W., Krader, P., Woodard, T., Holmes, D.E., VanPraagh, C.G., Lovley, D.R., 2007. *Geobacter pickeringii* sp. nov., *Geobacter argillaceus* sp. nov. and *Pelosinus fermentans* gen. nov., sp. nov., isolated from subsurface kaolin lenses. Int. J. Syst. Evol. Microbiol. 57 (1), 126–135. https://doi.org/10.1099/ijs.0.64221-0.

Shrestha, R., Cerna, K., Spanek, R., Bartak, D., Cernousek, T., Sevcu, A., 2022. The effect of low-pH concrete on microbial community development in bentonite suspensions as a model for microbial activity prediction in future nuclear waste repository. Sci. Total Environ. 808, 151861 https://doi.org/10.1016/j.scitotenv.2021.151861.

Smart, N.R., Reddy, B., Rance, A.P., Nixon, D.J., Frutschi, M., Bernier-Latmani, R., Diomidis, N., 2017. The anaerobic corrosion of carbon steel in compacted bentonite exposed to natural Opalinus Clay porewater containing native microbial populations. Corros. Eng. Sci. Technol. 52 (sup1), 101–112. https://doi.org/10.1080/1478422X.2017.1315233.

Stroes-Gascoyne, S., Hamon, C.J., Dixon, D.A., Kohle, C.L., Maak, P., 2006. The effects of dry density and porewater salinity on the physical and microbiological characteristics of compacted 100% bentonite. Mater. Res. Soc. Symp. Proc. 985 https://doi.org/10.1557/PROC-985-0985-NN13-02.

Stroes-Gascoyne, S., Hamon, C.J., Maak, P., Russell, S., 2010. The effects of the physical properties of highly compacted smectitic clay (bentonite) on the culturability of indigenous microorganisms. Appl. Clay Sci. 47 ((1–2), 155–162. https://doi.org/10.1016/j.clay.2008.06.010.

Thauer, R.K., Stackebrandt, E., Hamilton, W.A., 2007. Energy metabolism and phylogenetic diversity of sulphate-reducing bacteria. In: Sulphate-reducing Bacteria, pp. 1–38. https://doi.org/10.1017/cbo9780511541490.002.

Thijs, S., Op De Beeck, M., Beckers, B., Truyens, S., Stevens, V., Van Hamme, J.D., Weyens, N., Vangronsveld, J., 2017. Comparative evaluation of four bacteria-specific primer pairs for 16S rRNA gene surveys. Front. Microbiol. 8, 494. https://doi.org/10.3389/fmicb.2017.00494.

Vaïtilingom, M., Amato, P., Sancelme, M., Laj, P., Leriche, M., Delort, A.M., 2010. Contribution of microbial activity to carbon chemistry in clouds. Appl. Environ. Microbiol. 76 (1), 23–29. https://doi.org/10.1128/AEM.01127-09.

Villar, M.V., Fernández-Soler, J.M., Delgado Huertas, A., Reyes, E., Linares, J., Jiménez de Cisneros, C., Linares, J., Reyes, E., Delgado, A., Fernandez-Soler, J.M., Astudillo, J., 2006. The study of Spanish clays for their use as sealing materials in nuclear waste repositories: 20 years of progress. J. Iber. Geol. 32, 15–36.

Wagner, C.D., Riggs, W.M., Davis, L.E., Moulder, J.F., Muilenberg, G.E., 1979. Handbook of X-ray Photoelectron Spectroscopy: A Reference Book of Standard Data for Use in X-ray Photoelectron Spectroscopy. Perkin-Elmer Corporation, Eden Prairie, MN.

White, D.C., Sutton, S.D., Ringelberg, D.B., 1996. The genus *Sphingomonas*: physiology and ecology. Curr. Opin. Biotechnol. 7 (3), 301–306. https://doi.org/10.1016/S0958-1669(96)80034-6.

WNA. World Nuclear Association, 2021. Storage and disposal of radioactive waste. https://www.world-nuclear.org/.